Pipe depth measurement in small-scale backward erosion piping experiments

K. Vandenboer, V.M. van Beek & A. Bezuijen
Ghent University, Deltares, Ghent University and Deltares

Abstract: Backward erosion piping is an important failure mechanism for water-retaining structures, a phenomenon that results in the formation of shallow pipes at the interface of a sandy or silty foundation and a cohesive cover layer. Although the pipe depth reveals a lot of information on the backward erosion process, it has never been measured systematically. In this study we used a contactless laser triangulation sensor to measure the pipe depth during and after small-scale backward erosion experiments with a circular exit for three poorly graded sands with mean grain sizes varying from 0.155 mm to 0.544 mm. The pipes prove to be extremely shallow and the pipe depth close to the pipe tip is just large enough to let a particle through. As the pipe grows, the pipe depth increases due to scour and reallocation of grains, allowing for a higher flow rate and more grains to pass. Furthermore, the pipe often consists of a shallow part in the middle and deeper parts at the outside.

Keywords: Backward erosion piping, erosion, embankments, groundwater flow.

1 INTRODUCTION

1.1 Backward erosion piping

Backward erosion piping is an important failure mechanism for water-retaining structures founded on a sandy aquifer and covered by a cohesive blanket layer. A local disruption of the downstream top layer and sufficient head drop across the structure allows for erosion at that particular location (pipe initiation), resulting in the formation of shallow pipes in the sand layer (pipe progression). Eventually, the pipes form a direct connection between upstream and downstream, finally resulting in a (partial) collapse.

1.2 Current formulae

The safety factor regarding piping failure is often calculated according to Bligh's empirical rule (Bligh 1915), which is based on a large number of field failures and gives the maximum hydraulic load ΔH_{cr} as a function of the soil type and length of the construction. More recently, various design formulae were developed, which either predict piping susceptibility by correlating them to similar field cases in the past (Glynn, et al. 2012; Vorogushyn, et al. 2009), have a theoretical basis (Benjasuppatananan and Meehaln 2013; El Shamy and Aydin 2008; Ojha, et al. 2003; Schmertmann 2000), or a combined experimental-theoretical background (Schmertmann 2000; Sellmeijer, et al. 2011; Sellmeijer and Koenders 1991; Sellmeijer 1988; van Beek, et al. 2012).

1.2.1 Requirements for improvement of formula

None of the existing design formulae succeeds to correctly predict the piping susceptibility for a wide range of conditions. The large number of available models at present, with varying basic hypotheses indicates that the true incentive of backward erosion piping is not yet captured.

Up to now experimental studies have led to indispensable knowledge on key aspects of backward erosion piping either by analyzing the critical gradient or by studying the pipe formation in the sand bed: Hanses, et al. (1985), Miesel (1978) and van Beek, et al. (2011) identified the different phases involved and described the meandering character of the pipes. De Wit, et al. (1981) investigated the influence of the different downstream exit configurations on the critical gradient. Sellmeijer (1981) studied the erosion and fluidization in an outflow opening. Sellmeijer, et al. (2011) and van Beek, et al. (2010) considered a large number of sand types in order to identify the influence of relative density, uniformity, roundness, permeability and grain size on the susceptibility to backward erosion piping. Vandenboer, et al. (2013 and 2017) demonstrated that backward erosion piping should be treated as a three dimensional phenomenon rather than a two dimensional problem both in terms of groundwater flow and pipe development. van Beek, et al. (2014) studied the variation of pipe widths in relation to the grain size. Hanses, et al. (1985) and van Beek, et al. (2015) indicated progression is more likely to be driven by local detachment of the particles at the pipe tip, rather than erosion of particles at the pipe bottom.

An important parameter which has not yet been measured systematically is the depth of the pipe. However, the pipe depth is an important parameter in the research on backward erosion piping in several ways. Firstly, hydraulic analyses of water and sediment flow through the pipe and groundwater flow towards the pipe depend on the dimensions of the pipe and on the depth-to-width ratio of the pipe. Also, the variation of the pipe depth in time would indicate whether there is erosion at the pipe bottom (increasing depth) or not (constant depth). Moreover, implementation of incorrect estimations of the pipe depth and depth-to-width ratio in numerical simulations inevitably results in incorrect pore pressure distributions in the pipe and upstream of the pipe such that progress in understanding the piping process is again hindered.

This paper describes the measurement of the pipe depth in small-scale model tests for 3 different sands.

2 EXPERIMENTAL SETUP AND PROCEDURE

In laboratory conditions, the sandy aquifer is built in a pvc box, the cohesive water-retaining structure is replaced by an acrylate plate (see fig. 2.1) with a fixed circular opening representing a locally punctured top layer and the hydraulic gradient is applied by means of an upstream reservoir and a downstream overflow with adjustable head difference. The sand sample is prepared homogeneously at a relative density of more or less 80% in the box and has a total length of 0.4 m, a height of 0.1 m and a width of 0.3 m. The distance from upstream to the circular opening (seepage length) amounts 0.3 m. The hole type exit has a diameter of 5 mm and a height of 10 mm. A Perspex cylinder connects the hole type exit to the downstream reservoir.

A specific location in the setup can be described by its coordinates, see fig. 2.1a: the center of the hole type exit at the top of the sand bed is located at $x = 0$ m, $y = 0$ m, $z = 0$ m. All other locations vary between $x = -0.1$ m and $x = 0.3$ m (upstream), $y = -0.15$ m and $y = 0.15$ m and $z = 0$ m (top) and $z = 0.1$ m (bottom).

The initial hydraulic head difference ΔH of 0 cm is increased in steps of 0.5 cm every 5 minutes, as long as no erosion takes place. When the critical hydraulic head for initiation is exceeded, i.e. sand grains start to move and a pipe is formed, the hydraulic head is kept constant. If no erosion is observed for at least 5 minutes (equilibrium), the hydraulic head is increased again, usually resulting in progression of pipe growth. This process is repeated, until the 'critical hydraulic head for progression' ΔH_{crit} is exceeded, i.e. no equilibrium state is achieved and the pipe grows until it reaches the upstream filter and the test is stopped.

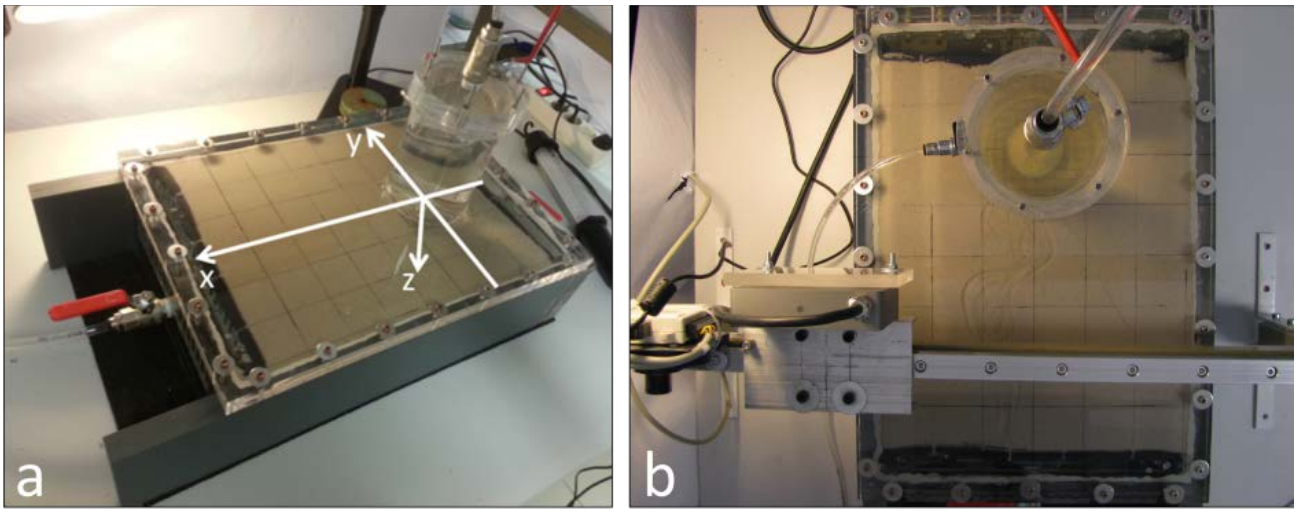

Figure 2.1. Experimental setup and pipe depth measurement device.

The pipe length is defined as the length of the projection of the pipe on the x-axis; the actual (meandering) pipe length is often longer. The eroded sand is deposited around the circular exit forming a crater. The flow rate is continuously measured by collecting the seepage water on a balance.

The replacement of the cohesive water-retaining structure by a transparent acrylate plate allows for measurement of the pipe depth through this cover. In this study a high-quality contactless laser triangulation sensor (resolution = 0.005 mm) is used which has been calibrated for its transition through the acrylate plate. By changing the position of the laser device, the pipe depth can be measured at different locations. Our setup is equipped with a one-dimensional linear guideway and position transducer in order to perform precise measurements in one direction (usually perpendicular to the pipe growth), see fig. 2.1b.

3 EXPERIMENTAL PROGRAM AND RESULTS

In this study, 3 different sand types were analyzed: 'Mol sand M34', 'Mol sand M32' and 'Cobo sand' (3 experiments for each sand type). These sand types are all poorly graded, and the mean grain size d_{50} varies from 0.155 mm to 0.544 mm. More characteristics can be found in table 3.1 Fig. 3.1 shows the critical head for progression ΔH_{crit} for the three sand types.

Table 3.1. Sand type characteristics.

	M34	M32	Cobo
d_{10} [mm]	0.128	0.172	0.248
d_{30} [mm]	0.142	0.212	0.389
d_{50} [mm]	0.155	0.251	0.544
d_{60} [mm]	0.166	0.271	0.646
d_{80} [mm]	0.209	0.311	1.680
C_u [-]	1.29	1.58	2.61
C_c [-]	0.94	0.96	0.95
k [m/s] (at RD 80%)	1.03E-04	3.28E-04	6.17E-04

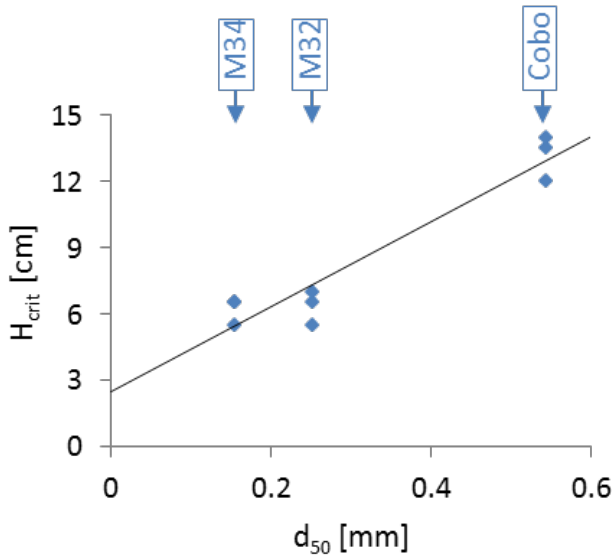

Figure 3.1. Critical hydraulic head for progression (ΔH_{cr}) as a function of mean grain size.

3.1 Online single-point measurements

During each experiment, the laser device continuously measures the pipe depth at a fixed location at x = 0.1 m, where the device is placed at the location where the center of the pipe is expected to pass. In this way the pipe depth variation in time is monitored from the moment the pipe reaches a length of 100 mm until the experiment finishes. This technique is called the 'online single-point measurement'.

Fig. 3.2a shows the top view of the pipe for one of the experiments on Mol sand M34. For this experiment, the online single point measurement is plotted in fig. 3.2b. The pipe reached a length of 100 mm after more or less 142 min, which is when the pipe depth at that location starts to increase. After 195 min, the pipe reaches the upstream filter and the experiment is ended. At that moment the pipe depth at x = 0.1 m is 0.778 mm. A lot of disturbance is observed, which is attributable to the passage of sand grains through the pipe underneath the laser measurement device.

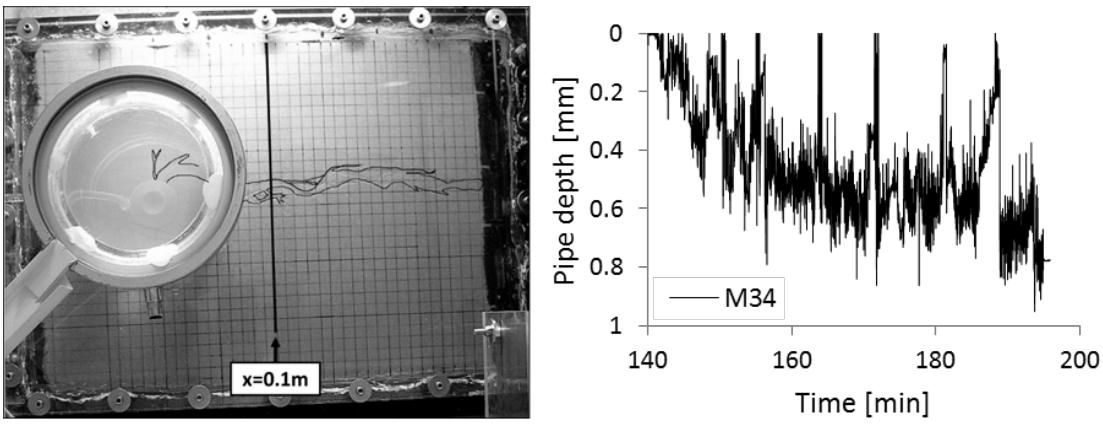

Figure 3.2. Photo at the end of an experiment on Mol sand M34 (a) and corresponding 'online single point measurement' at x=0.1 m (b).

The device is originally placed at the location where the center of the pipe is expected to pass. Often the position of the main streamline in the pipe, changes during the process, e.g. due to meandering or branching of the pipe. As a result, the measurement device is not always located at the center of the pipe but occasionally measures the pipe depth at an edge of the pipe where the depth may be larger or smaller

than in the center. Moreover, the pipe depth at a location might decrease as sand grains are deposited in a previously formed pipe channel. In fig. 3.2b the pipe depth does decrease occasionally for a short period, but the position of the pipe does not change considerably (thanks to the rather straight pipe course in this experiment, see fig. 3.2a) so sand grains keep flowing at the position of the laser measurement device and the pipe depth keeps evolving. This is not always the case and as a result, a horizontal lapse may appear in the 'online single point measurements', meaning that there is no pipe depth development, nor passage of sand grains at that point anymore. When this was observed during the experiments and it was considered to be unlikely that the pipe would retake its former course, the position of the laser measurement device was changed to the new main stream of the pipe, still at $x = 0.1$ m.

As the time scaling of the 'online single point measurements' is arbitrary for the different experiments, the pipe depth development (at $x = 0.1$ m) is plotted as a function of the pipe length, averaged for each sand type, see fig. 3.3. Note that the pipe is only a few sand grains deep and is larger in absolute sense for sands with larger grain sizes (although the pipe depth is more or less equal for M32 and M34 in the first half of the graph). The pipe depth slightly increases with the pipe length: since water concentrates towards the pipe, the flow rate at a certain point increases continuously causing scour and thus deepening and widening of the pipe cross section as the pipe gets longer and the distance from the monitored location to the pipe tip increases with time. Note that fig. 3.3 shows measurements at one position in the pipe cross section and although it seems that for Cobo sand the pipe depth does not increase significantly, this finding does not necessarily apply for the entire cross section.

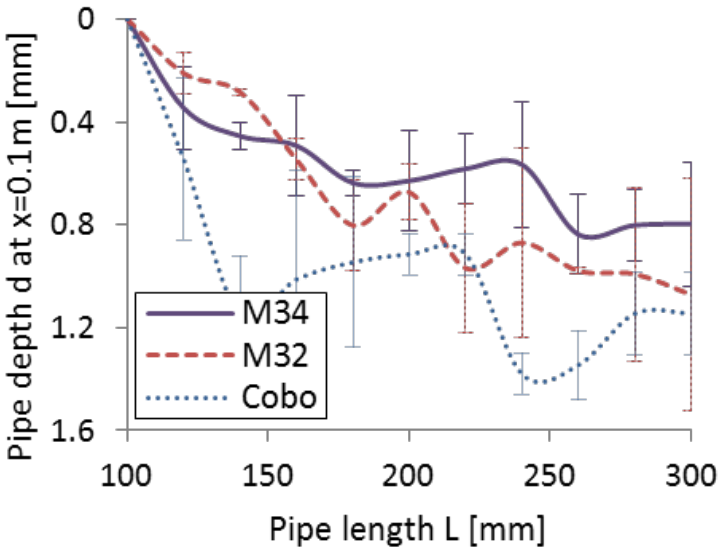

Figure 3.3. Online single point measurement at x=0.1 m for different sand types as a function of the pipe length.

3.2 Full measurement after test

The second technique 'full measurement after test' studies the complete depth profile of the pipe at the end of each test. When the pipe reaches the upstream filter, all taps are closed so the piping process stops. At that moment, the cross section of the pipe is measured at several locations along its length by passing the laser measurement device over the cross sections while recording both the pipe depth and the y-coordinate. In this way the depth variation along both the pipe length and the pipe width are surveyed. It is noted that the forced end of the piping process by closing the taps causes floating sand grains in the pipe to drop immediately. As a result, the measured pipe depth will be slightly smaller than the actual pipe depth during erosion. Fig. 3.4 shows examples of measured cross sections along the x-axis for the pipe in fig. 3.2a (M34 sand). When examining for example the cross section at $x = 0.1$ m, it is clear that the pipe is mainly located between $y = 22$ mm and $y = 45$ mm and consists of 2 deeper parts at the outsides and a shallow part in the middle. This is often observed, as meandering causes more scour at the

outside of a bend. In this case meandering evolved such that the outer bend at $x = 0.1$ m was originally at one side and later at the other side. Note that the scales of the x- and y-axes are not the same: the pipe is extremely shallow with an average depth of 0.39 mm (2.5 times the average grain size) and a width of 22.5 mm. In fig. 3.5 these cross sections are combined to a 3D surface. Despite the observed scatter, the geometry and location of the pipe are clearly observable.

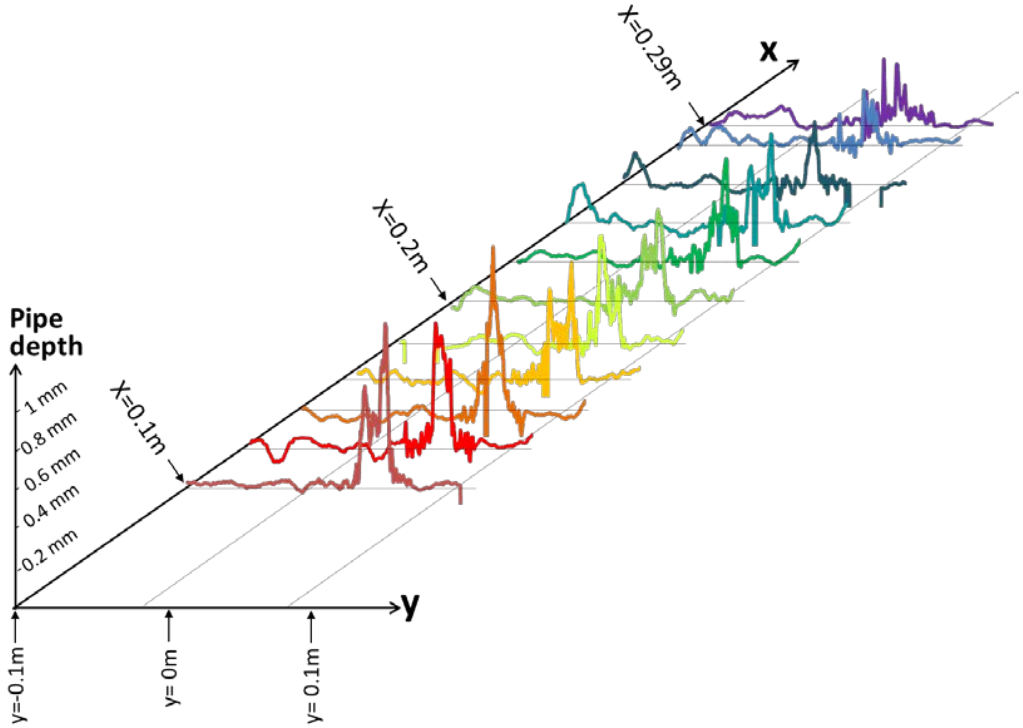

Figure 3.4. Pipe depth cross section measurements after test along x for M34 sand.

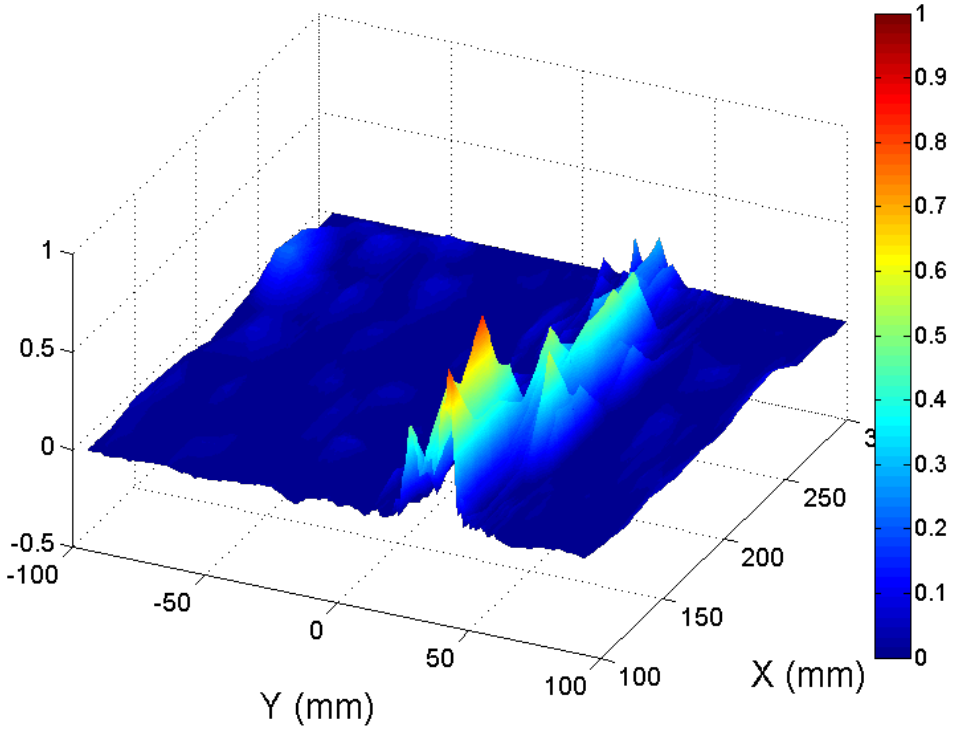

Figure 3.5. 3D surface of pipe depth cross section after test for M34 sand.

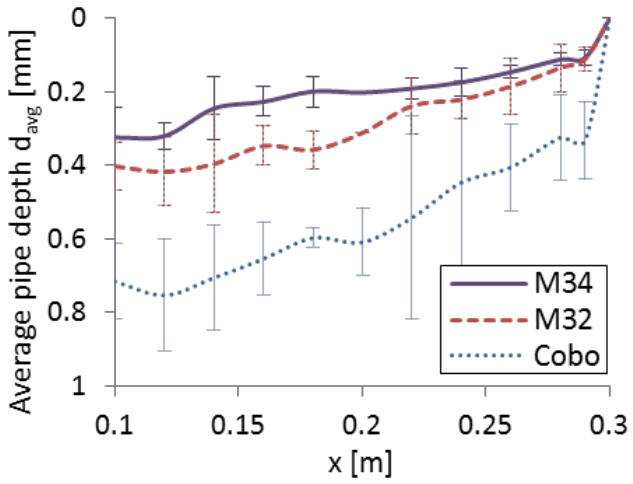

Figure 3.6. Full measurement of average pipe depth after test for each sand type.

In order to get a better idea of the evolution of pipe depth along the x-axis for the different sand types, the average pipe depth of each cross section d_{avg} is determined and averaged for all tests on the same sand type, see fig. 3.6. The pipe depth is larger for small x-values, as the pipe emerged early at that location and deepened in time, similar to fig. 3.3. Note that fig. 3.6 shows the average pipe depth of the cross section, implying that the pipe depth can be larger within the cross section (see fig. 3.4), which also explains that values smaller than 1 mm are observed close to $x = 0.3$ m, while fig. 3.3 shows the pipe depth at one location (often in the deepest part of the pipe).

4 SUMMARY AND CONCLUSIONS

A series of small-scale backward erosion experiments on three poorly graded sands with mean grain sizes varying from 0.155 mm to 0.544 mm was performed for which the pipe depth during and after the tests was measured using a contactless laser triangulation sensor.

During each test, the pipe depth evolution was continuously measured at a laterally fixed position at 0.1 m upstream from the exit hole. As the position of the main streamline in the pipe changes during the process, the measurements are not necessarily at the center or at the deepest part of the pipe. The first measurements are recorded when the pipe reaches a length of 0.1 m. Initially, the pipe depth increases gradually or suddenly after which it continues to increase gently.

After each experiment, the taps are closed and the cross section of the pipe was measured at several locations, giving an impression of the overall pipe geometry. Due to the forced end of the experiment, floating sand grains drop immediately which implies that the measured pipe depth may be slightly smaller than the actual pipe depth during erosion. The pipe depth increases suddenly to a certain value near the pipe tip, and increases gradually with the distance from the pipe tip. The pipes are extremely shallow, smaller than 1 mm at a length of 0.3 m for the three examined sand types. Additionally, the width to depth ratio is very large (order of 50). Due to meandering of the pipe, the pipe depth increases at the outer bends, often leading to a maximum pipe depth at either one or both edges of the pipe cross section.

The obtained information about the pipe cross section, the pipe depth variations and the absolute values of the pipe depth give valuable input for numerical simulations and analytical studies and may lead to further understanding of the phenomenon backward erosion piping.

Furthermore, the pipes are hard to detect in practice under an existing water-retaining structure. However, monitoring techniques with the aim do detect backward erosion piping and prevent failure can be optimized when keeping these extremely small pipe depths in mind.

Further research is needed to examine whether the pipe depths are in the same range for other sands and at larger scales and to determine the influence of diverse boundary conditions.

5 REFERENCES

Benjasuppatananan, S., and Meehaln, C.L. (2013). Analytical solutions for levee underseepage analysis: Straight and curved levee sections with an infinite blanket. *Geo-congress 2013:* 1129-1138.

Bligh, W.G. (1915). Submerged weirs founded on sand. *Dams and weirs: an analytical and practical treatise on gravity dams and weirs; arch and buttress dams, submerged weirs; and barrages, Chicago*: 151-179.

De Wit, J.M., Sellmeijer J.B., and Penning A. (1981). Laboratory testing on piping. *Tenth International Conference on Soil Mechanics and Foundation Engineering. Stockholm Sweden*: 517-520

El Shamy, U., and Aydin F. (2008). Multiscale modeling of flood-induced piping in river levees. *Journal of Geotechnical and Geoenvironmental Engineering* 134(9):1385-1398.

Glynn, E., Quinn M., and Kuszmaul J. (2012). Predicting piping potential along Middle mississippi river levees. International *conference on scour and erosion 2012, Paris, France*.

Hanses, U., Müller-Kirchenbauer H., and Savidis S. (1985). Zur Mechanik der rückschreitenden Erosion unter Deichen und Dämmen. *Bautechnik, Berlin, Germany: Wilhelm Ernst & Sohn* 62(5):163-169.

Miesel, D. (1978). Rückschreitende Erosion unter bindiger Deckschicht, *Deutsche Baugrundtagung, Berlin, Germany*

Ojha, C.S.P., Singh V.P., and Adrian D.D. (2003) Determination of critical head in soil piping. *Journal of Hydraulic Engineering, ASCE.* 129(7):511-518.

Schmertmann, J.H. (2000). The no-filter factor of safety against piping through sands. *Judgment and innovation at The Heritage and future of the geotechnical engineering profession, ASCE,*:68.

Sellmeijer, H., de la Cruz, J.L., van Beek, V.M., Knoeff, H. (2011). Fine-tuning of the backward erosion piping model through small-scale, medium-scale and IJkdijk experiments. *European Journal of Environmental and Civil Engineering* 15(8):1139-1154.

Sellmeijer, J.B., and Koenders M.A. (1991). A mathematical model for piping. *Applied Mathematical Modelling* 15(11-12):646-651.

Sellmeijer, J.B. (1981). Piping due to flow towards ditches and holes. *Flow and Transport in Porous Media: proceedings of Euromech 143, Delft, the Netherlands*

Sellmeijer, J.B. (1988). On the mechanism of piping under impervious structures, *PHD-thesis, TU Delft*.

Van Beek, V.M., Essen, H.M., Vandenboer, K., Bezuijen, A. (2015). Developments in modelling of backward erosion piping. *Géotechnique* 65(9):740-754.

Van Beek, V.M., Knoeff H., and Sellmeijer H. (2011). Observations on the process of backward erosion piping in small-, medium- and full-scale experiments. *European Journal of Environmental and Civil Engineering* 15(8):1115-1137.

Van Beek, V.M., Knoeff, J.G., Rietdijk, J., Sellmeijer, J.B, Lopez de la Cruz, J. (2010). Influence of sand and scale on the piping process: experiments and multivariate analysis. *Physical modelling in geotechnics. L.S. Springman*, London: Taylor and Francis group, 1221-1226..

Van Beek, V.M., Vandenboer K., and Bezuijen A. (2014). Influence of sand type on pipe development in small- and medium-scale experiments. *International conference on scour and erosion 2014. Perth, Australia.*

Van Beek, V.M., Yao, Q., Van, M., Barends, F. (2012). Validation of Sellmeijer's model for backward erosion piping under dikes on multiple sand layers. *International conference on scour and erosion 2012, Paris, France*: 543-550.

Vandenboer, K., van Beek V.M. and Bezuijen A. (2017). 3D character of backward erosion piping. *Géotechnique,* Advance online publication, doi:10.680/jgeot.16.P.091.

Vandenboer, K., van Beek V.M., and Bezuijen A. (2013). 3D FEM simulation of groudwater flow during backward erosion piping. *5th international Young Geotechnical Engineers' Conference, Paris, France*: 301-304.

Vorogushyn, S., Merz B., and Apel H. (2009). Development of dike fragility curves for piping and micro-instability breach mechanisms. *Natural Hazards and Earth System Sciences* 9(4):1383-1401.